Charles University in Prague
Faculty of Mathematics and Physics

SOLAR WIND DISCONTINUITIES AND THEIR INTERACTION WITH THE BOW SHOCK

Abstract of Doctoral Thesis

Andriy Koval

Department of Electronics and Vacuum Physics
V Holešovičkách 2, 180 00 Praha 8

Study branch: f-2 — Physics of Plasma and Ionized Media
Thesis supervisor: Prof. RNDr. Jana Šafránková, DrSc.
Prague 2006

Univerzita Karlova v Praze
Matematicko-fyzikální fakulta

DISKONTINUITY VE SLUNEČNÍM VĚTRU A JEJICH INTERAKCE S RÁZOVOU VLNOU

Autoreferát disertační práce

Andriy Koval

Katedra elektroniky a vakuové fyziky
V Holešovičkách 2, 180 00 Praha 8

Obor: f-2 — Fyzika plazmatu a ionizovaných prostředí
Školitel: Prof. RNDr. Jana Šafránková, DrSc.
Praha 2006

Disertační práce byla vypracována na základě výsledků vědecké práce na Katedře elektroniky a vakuové fyziky v letech 2002–2006 během mého doktorandského studia na Matematicko-fyzikální fakultě Univerzity Karlovy v Praze.

Uchazeč:
Mgr. Andriy Koval
Katedra elektroniky a vakuové fyziky MFF UK
V Holešovičkách 2
180 00 Praha 8

Školitel:
Prof. RNDr. Jana Šafránková, DrSc.
Katedra elektroniky a vakuové fyziky MFF UK
V Holešovičkách 2
180 00 Praha 8

Oponenti:
RNDr. M. Vandas, DrSc.
Astronomický ústav AV ČR
Boční II/1401
140 00 Praha 4

Prof. RNDr. Karel Kudela, DrSc.
Ústav experimentálnej fyziky SAV
Watsonova 47
043 53 Košice
Slovenská republika

Autoreferát byl rozeslán dne 2. dubna 2006.

Obhajoba se koná dne 2. května 2006 v 9:00 hodin před komisí pro obhajoby doktorských prací v oboru f-2, Fyzika plazmatu a ionizovaných prostředí, na MFF UK, Ke Karlovu 3, 121 16 Praha 2, v zasedací místnosti ÚDS.

S disertací je možno se seznámit na Útvaru doktorského studia MFF UK, Ke Karlovu 3, 121 16 Praha 2.

Předsedkyně RDSO f-2: Prof. RNDr. Jana Šafránková, DrSc.

Introduction

The interplanetary (IP) shocks and other types of discontinuities are a distinct feature of the solar wind. The prediction how the disturbances propagate in the solar wind, how they are modified in the bow shock region and through the magnetosheath, and how they affect the Earth's magnetosphere is a key question of present magnetospheric physics.

The first barrier on the way of solar wind discontinuities is the bow shock. Interactions of discontinuities with the bow shock lead to phenomena that have a significant influence on the Earth's magnetosphere. One of the most interesting of them are hot flow anomalies (HFAs) which are the results of the interplanetary magnetic filed (IMF) tangential discontinuity (TD) interactions with the bow shock and IP shocks which propagate into the magnetosheath and have a direct impact on the Earth's magnetosphere.

Hot flow anomalies

Regions of hot, highly deflected plasma often containing depressed magnetic field near the Earth's bow shock were discovered in the 1980s (*Schwartz et al.*, 1985; *Thomsen et al.*, 1986). The main observational features of HFAs include (*Schwartz*, 1995): (1) edge regions of enhanced magnetic field strength, density, and a slight increase in temperature. The outer edges of these enhancements are fast shocks generated by pressure enhancements within the core region. The inner edges of the enhancements are probably tangential discontinuities (*Paschmann et al.*, 1988). (2) The central regions of HFAs contain hot (10^6–10^7 K) plasma flowing significantly slower than the ambient solar wind in a direction highly deflected, in many cases nearly 90° from the Sun-Earth line. The flow velocity is often roughly tangential to the nominal bow shock shape (*Schwartz et al.*, 1988). (3) HFAs are associated with large changes in the IMF direction. Typically, the angle between the pre- and post-event fields is $\sim$70°.

It has been suggested that a formation of these events is due to the interaction of the bow shock with tangential or rotational discontinuities (*Schwartz et al.*, 1988; *Paschmann et al.*, 1988; *Thomas et al.*, 1991; *Thomsen et al.*, 1988). Kinetic simulations confirm that the interaction of IMF discontinuities with the bow shock can produce events with HFA characteristics (*Thomas et al.*, 1991; *Lin*, 1997). Using a test particle calculation associated with the interaction between the bow shock and TD, *Burgess* (1989) has shown that anomalous flows can be formed by specularly reflected ions moving upstream of the bow shock along a certain type of TD, where a motional electric field associated with the upstream bulk flow focuses reflected ions towards TD from either side of the TD.

Schwartz et al. (2000) investigating a set of 30 HFAs have defined conditions for the HFA formation: (1) an interplanetary current sheet with a motional electric field which points towards it on at least one side; (2) current sheets whose normals make a large cone angle with the sunward direction; (3) tangential discontinuities (probably). Suggesting that all TDs above 60° of the cone angle with towards electric field on at least one side result in HFAs, the authors have estimated an occurrence rate of $\sim$3 HFAs per day which is consistent with observations.

Such HFA features should be swept downstream, however, only a few HFAs have been observed in the magnetosheath (*Paschmann et al.*, 1988; *Thomsen et al.*, 1988; *Schwartz et al.*, 1988; *Šafránková et al.*, 2000). For example, *Šafránková et al.* (2000) suggests a

negligible evolution of HFAs in the magnetosheath. The authors have pointed out that HFAs must be rather frequent in the central magnetosheath and little evidence for them in the literature may be attributed to the difficulties of distinguishing them among other phenomena in a highly disturbed magnetosheath flow. These magnetosheath HFAs exhibit a clear tendency to occur predominantly during periods of enhanced solar wind speed. *Šafránková et al.* (2000) have also shown a double structure of some magnetosheath HFAs which is probably connected with the mechanism of the HFA formation in front of the bow shock. Magnetosheath double HFAs are distinguished by the ion flux enhancement that divides a core region into two parts. Consecutive study (*Šafránková et al.*, 2002) has pointed out that plasma parameters inside this enhancement are similar to those in the surrounding undisturbed magnetosheath. The principal rotation of the magnetic field from pre-event to post-event orientations occurs inside the HFA core and not on its boundaries. This field rotation usually, but not always, coincides with the center of the flux enhancement.

Although almost all reported magnetosheath events have been identified near the bow shock, they may influence significantly the magnetosphere. *Sibeck et al.* (1999) have demonstrated a remarkable magnetospheric response to an IMF tangential discontinuity which resulted in a sunward magnetopause displacement exceeding 5 R_E. The authors have shown that the underlying IMF TD was not unaccompanied by any significant plasma variation and was itself totally unremarkable, and conclude that such transient but dramatic disturbances of the magnetosphere are common.

Propagation of interplanetary shocks through the solar wind and magnetosheath

IP shocks in the solar wind are generally assumed to be planar on the scale size of the Earth's magnetosphere (e.g., *Russell et al.*, 2000). *Russell et al.* (2000) analyzed a single IP shock with four solar wind spacecraft and found that normals calculated from the data of three of them were consistent with the planarity assumption (with the accuracy of the travel time estimates).

However, a deviation from the planarity has been also reported (e.g., *Russell et al.*, 1983; *Šafránková et al.*, 1998; *Szabo et al.*, 2001; *Szabo*, 2005). For example, *Szabo et al.* (2001) analyzed six magnetic cloud driven IP shocks, each observed by two spacecraft located in the solar wind. The calculated local shock front orientations indicate that IP shocks driven by slow and small magnetic clouds have a significant level of corrugation, mostly limited to the plane perpendicular to the cloud axis. On the other hand, fast and large magnetic clouds, if they are encountered close to the center, drive nearly planar shocks. Also, *Szabo* (2005) analyzed an IP shock observed by five spacecraft in the solar wind. The author have calculated local shock normals at positions of three spacecraft (Wind, ACE, and IMP 8). These local normals were then compared with five global shock orientations calculated from four-spacecraft positions and times of the shock passages. Analyzing the differences in the shock normal orientations, *Szabo* (2005) has concluded that there exist small scale (few R_E) ripples or corrugation on the surface of the shock.

The interaction of IP shocks with the bow shock and their transmission through the magnetosheath have been studied by gasdynamic (e.g., *Dryer*, 1973; *Spreiter and Stahara*, 1992) and MHD (e.g., *Whang*, 1991; *Yan and Lee*, 1996) modeling. The gasdy-

namic models allow the generation and propagation of only fast forward shocks in the magnetosheath, thus they find only a single, fast mode pressure pulse (or a fast shock in the supersonic flanks) propagating through the magnetosheath. On the other hand, MHD models predict a more complicated scenario. For example, the one-dimensional MHD modeling of *Yan and Lee* (1996) suggests that, if an incident forward shock transmits through the bow shock, a fast shock, a slow expansion wave, a slow shock, and a contact discontinuity are generated downstream of the bow shock. If the incident shock is a reverse shock, the generated fast shock becomes a fast expansion wave.

Parameters of a shock propagating through the magnetosheath are essential for prediction of the shock arrival to the magnetosphere. The gasdynamic modeling of *Spreiter and Stahara* (1992) suggests that the IP shock remains nearly planar as it moves through the magnetosheath and that the extent of the transition flow region is relatively short. This prediction is supported by observations reported by *Szabo et al.* (2000). Moreover, *Szabo* (2004) analyzed IP shock surface normals and propagation speeds in the solar wind and estimated the predicted arrival times in the MSH. They have concluded that there is no clear dependence of the arrival times on the spacecraft separation from the Sun-Earth line indicating no systematic deformation in the pressure front surface.

However, the difference between the shock parameters in the magnetosheath and those in the solar wind have also been reported. For example, *Zhuang et al.* (1981) analyzed propagation of three IP shocks for which measurements of ISEE 1, 2, and 3 were available in the solar wind and magnetosphere. Using the *Zhuang and Russell* (1981) model of the magnetosheath, they concluded that an IP shock front does not propagate as a plane in the magnetosheath: the different elements of the front have different velocities and orientations. More recently, *Villante et al.* (2004) examined 20 fast forward IP shocks detected by Wind in the solar wind in order to determine propagation speeds of shock-associated disturbances in the magnetosheath. They found the propagation velocity for shock-associated disturbances through the magnetosheath to be $\sim$1/3–1/4 of the solar wind shock speed. However, their study is based on the solar wind and ground observations only, assuming a transit time between the magnetopause and the Earth's surface of $\sim$1–2 min.

The aims of the thesis

From a short overview of previous HFA investigations it follows that, despite a significant progress made in an HFA structure and gradual evolution studies, there are many problems in our understanding. Among them are: (1) conditions that lead to the ion flux enhancement on both or only one edge of HFA, (2) a nature of double HFA formation, (3) the distinction in influence of a motional electric field oriented towards the IMF TD plane on both or only one side on an HFA formation, (4) the relationship between the deflected particle flow inside HFA and orientation of the original IMF TD. Thus our attention was devoted to one of these problems, namely the investigation of the particle flow inside HFA and its relationship to the orientation of the IMF TD. For this study, we used the high-time resolution data of ion fluxes measured by Faraday's cups of the omnidirectional plasma sensor VDP onboard the Interball-1 spacecraft.

On the other hand, previous studies of the IP shock propagation through the magnetosheath do not come to a clear conclusion on the influence of an IP shock interaction

with the bow shock on parameters of the resulting shock or shock-like discontinuity in the magnetosheath. This encouraged us for a more detailed investigation of this phenomenon. The complex study of IP shock propagation through the magnetosheath can be divided into following tasks:

- To compare IP shock properties in the solar wind with properties of the resulting shock in the magnetosheath.
- To compare a propagation of the IP shock through the magnetosheath with their MHD predictions.
- To analyze magnetic field and plasma parameter profiles across a shock in the magnetosheath and compare them with the same profiles in the solar wind and with predictions of MHD models.

For the study of IP shock propagation through the magnetosheath, we primarily focused on analysis of events when the shock arrival was observed by at least four spacecraft in the solar wind and, assuming planar shock geometry, we could directly calculate global shock characteristics from the times of a shock arrival to a particular spacecraft. Since IP shocks are rather rare in the solar wind and suggested way of data processing requires multi-point observations, we started with a survey of available solar wind and magnetosheath observations and created a database of observed shocks for a period from 1995 to 1999 when the required number of spacecraft was available.

Instrumentation and data processing

Our study is based on simultaneous observations of several spacecraft that operated as distant solar wind monitors (SOHO, Wind, ACE), or were located either in a close vicinity of the Earth's bow shock (IMP 8, Geotail, Interball-1/MAGION-4) or in the magnetosheath (Geotail, Interball-1/MAGION-4).

We used data of Wind magnetic field (*Lepping et al.*, 1995) and plasma (*Ogilvie et al.*, 1995; *Lin et al.*, 1995) instruments, ACE magnetic field (*Smith et al.*, 1998) and plasma (*McComas et al.*, 1998) instruments, SOHO plasma instrument (*Ipavich et al.*, 1998), Geotail magnetic field (*Kokubun et al.*, 1994) and plasma (*Frank et al.*, 1994) instruments, IMP 8 magnetic field (ftp://nssdcftp.gsfc.nasa.gov/spacecraft_data/imp/imp8/mag/ (A. Szabo and R. P. Lepping, NASA GSFC)) and plasma (*Bellomo and Mavretic*, 1978) instruments, Interball-1 magnetic field (*Klimov et al.*, 1997; *Nozdrachev et al.*, 1998) and ion flux (*Šafránková et al.*, 1997) instruments, MAGION-4 magnetic field (*Ciobanu and Moldovanu*, 1995) and ion flux (*Šafránková et al.*, 1997) instruments.

Among the above listed spacecraft, Interball-1 has some advantages for our study: (1) trajectories of the spacecraft are suitable for study of interaction of solar wind discontinuities with the Earth's bow shock and their propagation in the magnetosheath because, being launched into a highly elongated polar orbit, Interball-1 passed through the magnetosheath twice per orbit lasting four days; (2) the spacecraft provided the highest time resolution of plasma and magnetic filed measurements.

There were two devices for plasma measurements onboard Interball-1 — ion energy spectrometer (CORALL) and ion flux detector VDP. However, time resolution of

CORALL measurements were $\sim$2 minutes and geometry of this device did not allow to determine solar wind parameters and thus we were forced to use the ion fluxes measured by the VDP instrument. To determine particular ion flow parameters (three components of the velocity vector, temperature, and density) from the ion flux measurements, we have developed new methods based on a comparison of actual observations with model results of the instrumental response for various sets of ion flow parameters assuming an isotropic Maxwellian velocity distribution. These methods are appropriate for high ion-temperature regions (e.g., magnetosheath or HFA) and allow to determine ion flow parameters with a high-time resolution up to 1 s.

Results

Particle flows in hot flow anomalies

The study of particle flows inside HFAs (*Koval et al.*, 2005b) [A2] is based on analysis of three HFAs in Interball-1/MAGION-4 solar wind measurements.

Figure 1 presents one of these events observed on May 20, 1996 by Interball-1 located in the vicinity of the bow shock at (14, 1.8, -4.7) R_E in the GSE coordinate system. Four top left panels in Figure 1 show Interball-1 ion fluxes and magnetic field. The observed event can be distinguished as two sharp jumps of the magnetic field strength (at $\sim$2322 and $\sim$2328 UT) from about 5 to $\sim$27 nT. The region bounded by these enhancements exhibits a very strong ion flow observed by FCs oriented perpendicularly to the Sun-Earth line, whereas the anti-sunward ion flow is highly depressed. The comparison of magnetic field components prior and after the event reveals that although the magnetic field strength remained nearly unchanged, the vector rotated on a large angle.

During the studied time interval, the solar wind and IMF conditions were monitoring by Wind located far upstream at (113, -29, -5.2) R_E. Its IMF and plasma measurements are shown in three bottom left panels in Figure 1. The considered time interval does not contain any sharp change in the solar wind dynamic pressure confirming our suggestion of an IMF origin of the event. Moreover, the similarity of Interball-1 measurements after the event with those of Wind following a distinct discontinuity at 2258 UT suggests that this discontinuity can be considered as a cause of the observed disturbance. The normal of the discontinuity calculated from the WIND data by the cross product of the magnetic field vectors on both sides of the discontinuity is $\boldsymbol{n}$=(0, 0.14, -0.99). A motional electric field is oriented towards the plane of the discontinuity on one side.

Using the method for the determination of ion flow parameters from the ion fluxes measured by the VDP instrument onboard Interball-1, we have calculated the ratio of bulk to thermal velocities (V/V_{th}) and two angles (θ and ϕ) that define the ion flow direction. Right part of Figure 1 (panels c, d, e) presents these parameters with 1-s time resolution for the time interval corresponding to the discontinuity. There is a sharp drop in a value of V/V_{th} from more than 4 to less than 1 (core region) and simultaneous significant changes of the ion flow direction at the discontinuity boundaries as well as along the core region.

Since the plane of the discontinuity is almost parallel to the XY_{GSE} plane, we can neglect its motion along the bow shock surface. Thus, we can calculate the angle (α) between the plane of the discontinuity and the ion flow direction with 1-s time resolution

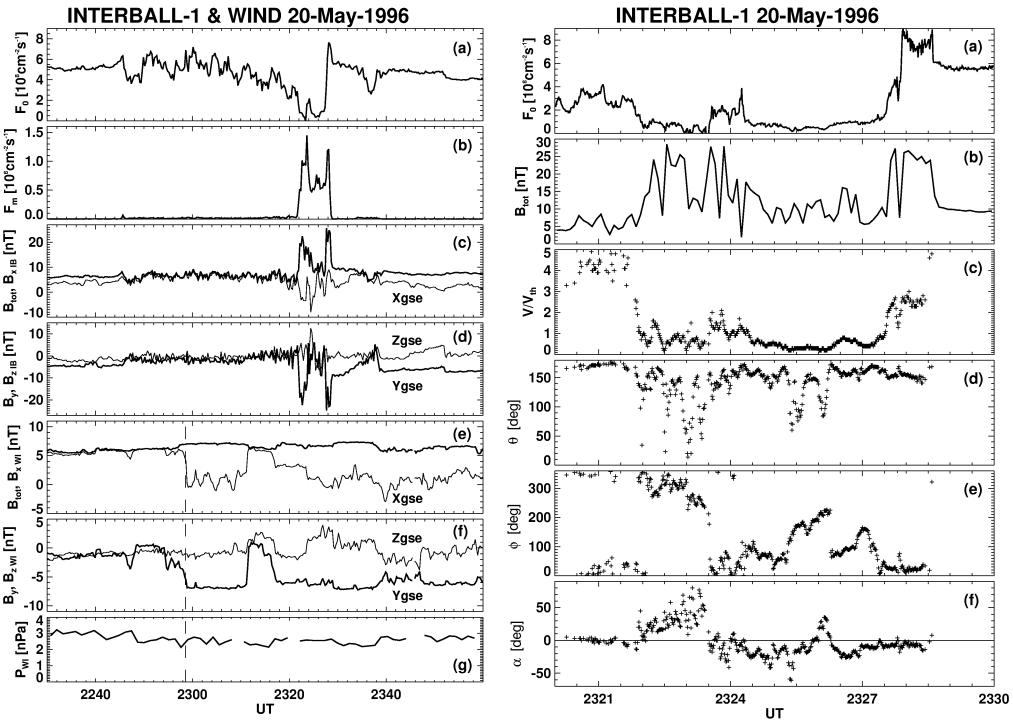

Figure 1: *Left*: A summary plot of the solar wind HFA observed by Interball-1 and IMF TD observed by Wind. (a) The F_0 (Interball-1 ion flux in the anti-sunward direction), (b) F_m (Interball-1 ion flux in the plane perpendicular to the Sun-Earth line), (c) $B_{tot\ IB}$ (Interball-1 magnetic field magnitude), $B_{x\ IB}$, (d) $B_{y\ IB}$, $B_{z\ IB}$ (Interball-1 magnetic field components), (e) $B_{tot\ WI}$ (Wind magnetic field magnitude), $B_{x\ WI}$, (f) $B_{y\ WI}$, $B_{z\ WI}$ (Wind magnetic field components), (g) P_{WI} (Wind dynamic pressure). ***Right***: Interball-1 HFA observations. (a) F_0 (ion flux in the anti-sunward direction), (b) B_{tot} (magnetic field magnitude), (c) V/V_{th} (ratio of bulk to thermal velocities), (d) θ (angle between the ion flow vector and positive X direction), (e) ϕ (angle between the positive Y direction and the projection of the ion flow vector onto the YZ plane counted toward the positive Z direction), (f) α (angle between the ion flow vector and the plane of the discontinuity in the discontinuity frame of reference).

(bottom right panel in Figure 1). A positive value of the angle corresponds to the southward, while a negative value to the northward ion flow. The ion flow is rather deflected from the discontinuity plane with an angle up to 70° which is roughly tangential to the bow shock surface at the leading edge, while is almost aligned with the plane at its trailing edge. The core region (2324:30-2327:20 UT) is characterized by a moderate value of this angle that does not exceed 20°.

Although the IMF TD has all features required for a HFA creation, the resulting disturbance is not a typical HFA. It is bounded by magnetic field enhancements on both sides but only the trailing edge has characteristics of the fast shock. The compression of the field on the trailing edge is accompanied with compression and slight heating of the plasma. The V/Vth ratio is about 2.6 and the total ion flux is enhanced by a factor of 1.5 with respect to the undisturbed solar wind observed after 2328:30 UT. On the other hand, the space with enhanced magnetic field on the leading edge of the disturbance (2322-

2324 UT) is filled with hot and tenuous plasma similar to that in the core region. The only difference between these two plasmas is the flow direction. It is deflected from the discontinuity plane towards south inside the enhancement, whereas northward declination characterizes the core region. However, the ratio of bulk to thermal velocities is very low and indicates nearly standing plasma in the core region.

Our analysis of the flow directions in the described HFA and two other HFAs (presented in *Koval et al.* (2005b) [A2]) reveals that the deflection from the original solar wind velocity starts in bounding density enhancements if they exhibit fast shock features. The flow direction inside the core region can be determined only approximately because the bulk speed is comparable or even smaller than the thermal speed. Nevertheless, the flow velocity lay nearly in the discontinuity plane in all analyzed events. The declinations up to $\pm 20^\circ$ can be probably attributed to the fluctuations of the IMF direction changing slightly the normal of the discontinuity plane. This flow carries a large amount of plasma in direction different from that of the undisturbed solar wind. However, this flow originates and should be terminated in the solar wind. One would expect to see a kind of transient process at these point but none of analyzed cases exhibits such features. It suggests that the HFA cavity is probably highly elongated in the direction of the discontinuity plane. A highly elongated shape can explain very different duration of HFA observations. HFA is crossed by the satellite in an arbitrary direction and the velocity of a HFA motion with respect to the bow shock is given by the orientation of the seed TD. The duration of HFAs in satellite observations can range from seconds to tens of minutes.

Modification of an interplanetary shock in the solar wind and magnetosheath

The paper of *Koval et al.* (2004) [A3] shows an example that demonstrates possibility of evolution of an IP shock while propagating through the solar wind and its transformation into another type of the MHD shock after an interaction with the Earth's bow shock.

On January 31, 1998, Wind and ACE identified an IP shock far upstream in the solar wind (Figure 2 where projections of spacecraft locations onto the ecliptic plane are presented). The shock was registered first by Wind at 1553:46 UT and latter by ACE at 1600:31 UT. Wind and ACE observations corresponding to these times are presented in left panels in Figure 3. The arrival of the shock can be clearly seen in magnetic field and plasma data. It is characterized by an abrupt increase of the IMF magnitude as well as the solar wind speed and density. According to changes of these parameters, the discontinuity can be classified as a fast forward shock. It propagated through the solar wind to the Earth's bow shock vicinity where IMP 8 identified a corresponding disturbance (two bottom left panels in Figure 3). However, the profile of the disturbance observed near the Earth's bow shock differs significantly from that of the initial shock. Propagating through the solar wind, the shock evolves into a slow IMF rotation which is registered by IMP 8. A small-amplitude sharp IMF change at 1642 UT is supposed to be a signature of the initial shock observed at L1.

The IMF rotation interacts with the Earth's bow shock and produces a new shock-like discontinuity in the magnetosheath where it is observed by Interball-1 (Figure 3, right panels). Two top right panels in Figure 3 show magnetic field measurements corresponding to the discontinuity arrival. The discontinuity is clearly identified by a very sharp

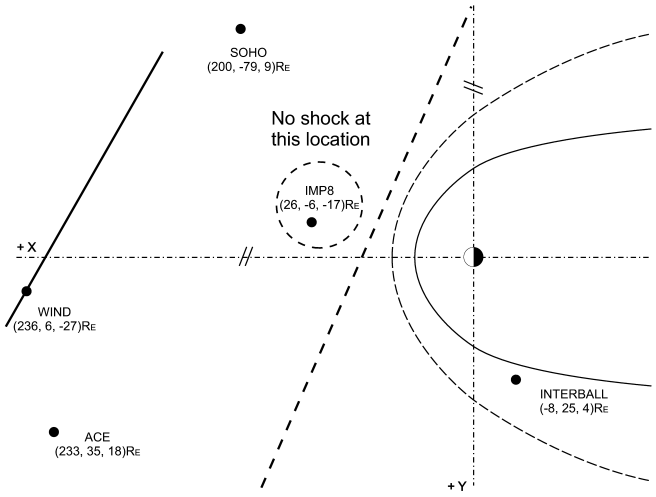

Figure 2: Projections of spacecraft locations onto the ecliptic plane and shock plane estimations. The global shock orientation calculated from the times of the shock arrival to four spacecraft is denoted by a dashed line while a local shock orientation at the Wind location calculated using Rankine-Hugoniot conservation equations is denoted by a heavy line.

increase of the magnetic field magnitude at 1649:41 UT. The other right panels in Figure 3 present the ion anti-sunward flux, proton number density, and speed as well as ion and electron spectra. Since the increase of the magnetic field magnitude is accompanied by the decrease of the density, the discontinuity in Interball-1 data exhibits the features of a slow reverse shock despite the fact that the initial solar wind shock has all attributes of a fast forward shock.

Deformation of interplanetary shock fronts in the magnetosheath

In the study (*Koval et al.*, 2005c,d) [A4, A5], we discuss possible deformations of an IP shock front using an example of a shock observed by four spacecraft in the solar wind and by one spacecraft in the magnetosheath. The case study is supplemented with a small statistical study of similar shocks.

The passage of the IP shock was registered in late May 17 and early May 18, 1999 by four spacecraft (SOHO, ACE, Wind, and Interball-1) located in the solar wind; Geotail, located in the magnetosheath, observed a corresponding shock-like discontinuity. Figure 4 shows the spacecraft geometry and model positions of the Earth's bow shock (*Jeřáb et al.*, 2005) and magnetopause (*Petrinec and Russell*, 1996).

ACE, Wind, and Interball-1 observations of the IP shock passage are presented in the six top panels in Figure 5. The simultaneous jumps of the magnetic field magnitude, proton number density, and bulk velocity indicate that the observed IP shock is a fast forward shock. The three bottom panels in Figure 5 present Geotail magnetosheath observations.

To study the propagation of the IP shock toward the magnetosheath, the shock normal orientation, and speed in the solar wind should be determined. We used magnetic field and plasma data from the ACE and Wind spacecraft and applied the Rankine-Hugoniot relations to determine local shock normals and speeds. With measurements from four

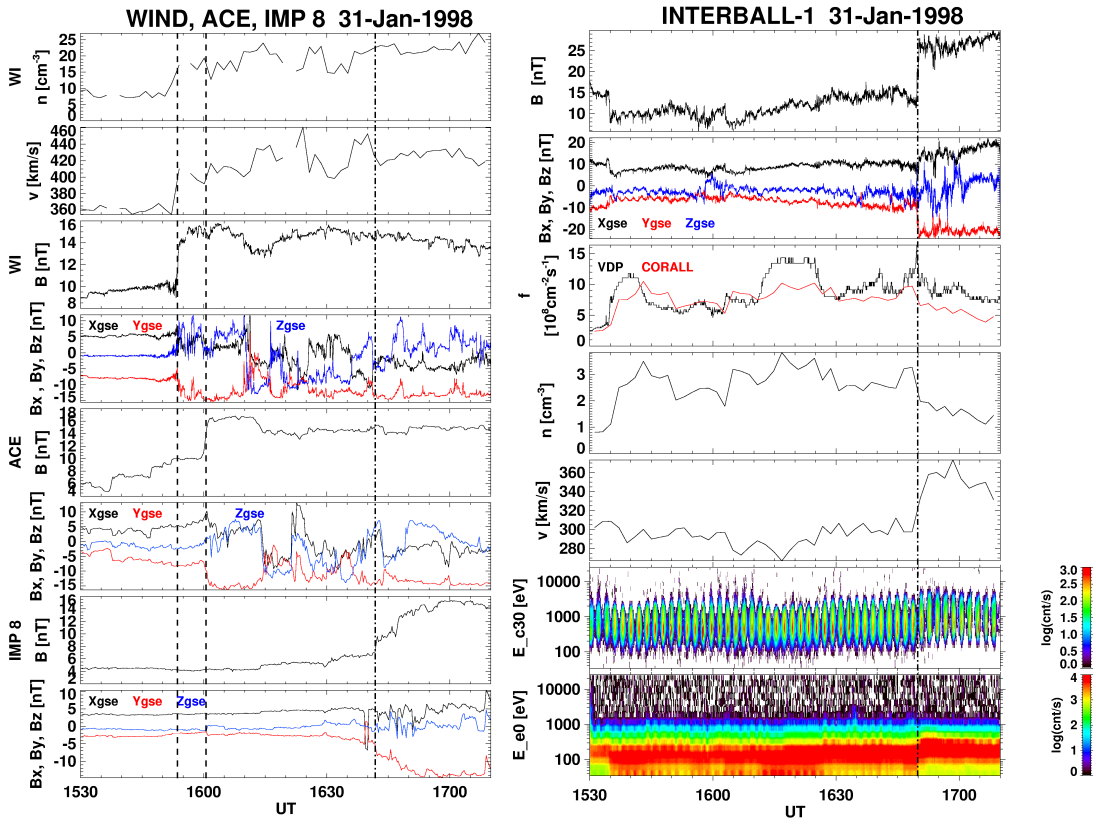

Figure 3: Observations of an IP shock by Wind (WI), ACE, and IMP 8 in the solar wind (*left*) and a corresponding disturbance observed by Interball-1 in the magnetosheath (*right*). Left panels: solar wind number density and speed measured by Wind and IMF measured by Wind, ACE, and IMP 8; Right panels: magnetosheath magnetic field, ion anti-sunward flux, proton number density and speed, ion and electron spectra.

spacecraft located in the solar wind, we can also estimate the shock normal and speed as global shock parameters from the times of shock arrival at each spacecraft. Table 1 presents the derived shock parameters and Figure 4 shows the shock orientations: local shock normals computed from the Rankine-Hugoniot relations are denoted by arrows, while the global shock plane computed from the shock arrival times at each spacecraft is represented by a dashed line.

The Rankine-Hugoniot relations were also applied to magnetosheath measurements of Geotail and the resulted parameters are presented in Table 1. The comparison of the shock parameters reveals that the shock orientation in the magnetosheath differs significantly from that in the solar wind and the IP shock propagates much slower through the magnetosheath. However, the shock speeds in the plasma frame are almost equal in the solar wind and magnetosheath (Table 1). Therefore, the decrease of the shock speed in the magnetosheath can be attributed to a smaller bulk flow velocity.

In order to confirm the results of the shock deceleration in the magnetosheath, we have carried out a statistical study of a small number of similar shocks observed in the solar wind and magnetosheath.

The shock parameters in the solar wind can be determined from the magnetic filed

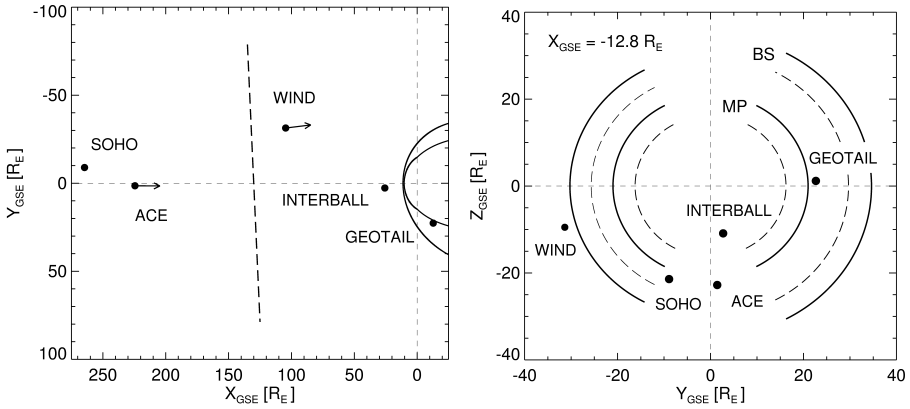

Figure 4: Projection of the spacecraft locations onto the ecliptic plane (a) and onto the YZ_{GSE} plane at $X = -12.8R_E$ (b). The *Jeřáb et al.* (2005) and *Petrinec and Russell* (1996) models were used to determine Earth's bow shock and magnetopause locations before (solid lines) and after (dashed lines) the shock arrival.

Technique	Shock Normal	Speed[1]	Speed[2]	Ma	Mf
ACE R-H	(-0.990, 0.005, 0.139)	440.2	99.8	2.28	2.15
Wind R-H	(-0.996, -0.087, -0.003)	450.4	99.9	2.46	2.30
4 S/C Timing	(-0.985, -0.063, -0.159)	429.8	83.8	2.01	1.89
Geotail R-H	(-0.961, 0.276, 0.000)	376.0	96.9	1.92	1.64

Table 1: Parameters of the IP shock (shock normals, speeds in km/s ([1] in Earth's and [2] plasma frames of reference), Alfvénic, and fast magnetosonic Mach numbers in the solar wind and magnetosheath.

and plasma parameters measured by a single spacecraft during the shock passage. However, we believe that the most reliable and least noisy parameters that can be derived from spacecraft observations are the time of the shock arrival at the spacecraft and its coordinates. The determination of shock parameters from the timing of observations requires the same shock be identified by at least four solar wind spacecraft and this requirement limits the number of IP shocks available for analysis. The number of shocks that can be studied is further decreased by the need to have at least one spacecraft operating in the magnetosheath as well as four in the solar wind.

Among about 120 IP shocks observed in the solar wind for the time interval from 1995–1999, we have identified 10 fast forward shocks which satisfy these criteria. However, for each of these events, there is no a complete set of magnetic filed and plasma parameters measured in the magnetosheath that precludes us from the direct comparison of shock parameters in the solar wind and magnetosheath. Therefore, we have computed the differences between the times predicted using shock orientations and speeds calculated in the solar wind and the times of the shock arrivals in the magnetosheath.

Since the magnetosheath is relatively thin compared to the bow shock displacement due to pressure jumps across IP shocks, we divided all events into two groups which are determined by the magnetosheath observations. The first group contains events in which the spacecraft remains in the magnetosheath for a long time prior to and after the IP shock arrival (the event described above is an example). The second group contains

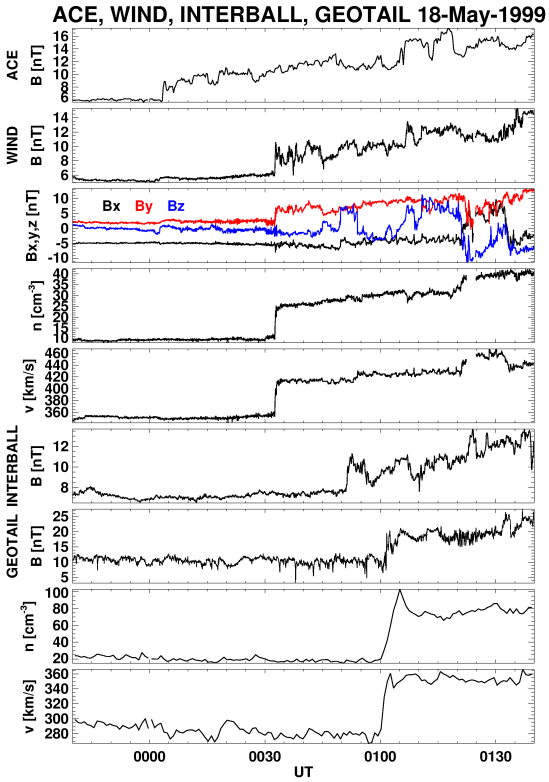

Figure 5: Observations of the IP shock passage by ACE, Wind, and Interball-1 in the solar wind and by Geotail in the magnetosheath. From top to bottom: ACE IMF magnitude, Wind IMF magnitude, and three IMF components, the Wind density and solar wind velocity, Interball-1 IMF magnitude, Geotail magnetic field magnitude, the density, and velocity.

events where the magnetosheath spacecraft crossed the bow shock within several minutes after the IP shock passed the spacecraft. Observations in the first group are likely closer to the magnetopause than those of the second group. The calculated delay times of IP shocks in the magnetosheath are plotted in Figure 6 as a function of the distance of the magnetosheath spacecraft from the magnetopause prior the IP shock arrival. The two groups of observations are distinguished by different symbols. Error bars reflect uncertainties of the shock determination due to the time resolution of the measurements onboard the spacecraft used for the particular calculation. The figure shows that almost all computed delays are positive which corresponds to deceleration of shocks. The only negative delay is small and belongs to the shock with the highest Alfvénic Mach number ($M_A \sim$5) in our set. However, the expected increase of the delay for the points closer to the magnetopause is not confirmed, perhaps because the number of points is small and their spread is large. Moreover, the magnetosheath observations significantly differ in the X_{GSE} coordinate.

MHD modeling of IP shock propagation through the magnetosheath

The observed shock deceleration in the magnetosheath disagrees with the gasdynamic model predictions of *Spreiter and Stahara* (1992). For this reason, we adapted the 3-D

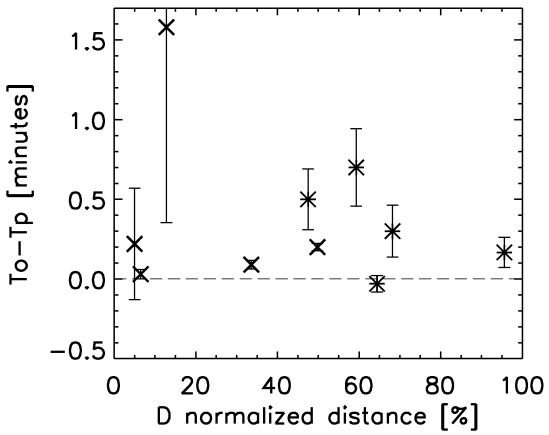

Figure 6: Differences between observed and predicted times ($To - Tp$) of IP shock arrival in the magnetosheath as a function of D, the ratio of the radial distance of the spacecraft from the model magnetopause (*Petrinec and Russell*, 1996) to the magnetosheath thickness (crosses – IP shock observations deep within the magnetosheath; asterisks — magnetosheath shock arrivals followed by bow shock crossings). For detail description of error bars see the text.

MHD model of solar wind flow around a blunt obstacle (*Samsonov and Hubert*, 2004) to allow for the propagation of a disturbance along the simulation box. We have analyzed several runs where a discontinuity satisfying the fast shock jump conditions propagated toward the Earth (*Koval et al.*, 2005c) [A4]. Figure 7 illustrates the model results, showing the magnetic field intensity in the equatorial plane 3 and 4.5 minutes after a weak shock launch (see the Figure 7 caption for shock model parameters). The magnetic field strength is scaled to the undisturbed value at each point of the plot. The black line shows the location of the steepest gradient, which we presume is the bow shock. The IP shock can be easily distinguished on the plot as the boundary between the dark and light areas. The narrow light regions near the bow shock result from the bow shock displacement and our normalization because the magnetic field downstream of the IP shock is lower than that in the subsolar magnetosheath.

The figure reveals that the shock propagates as a plane in the solar wind but its surface is curved in the magnetosheath. The shock speed just downstream of the bow shock is the same as that in the solar wind but it is significantly lower in the vicinity of the magnetopause. The time delay resulting from this deceleration is about $\sim$25 s after $\sim$3 minutes of IP shock propagation through the magnetosheath.

Because the results of the MHD model qualitatively agree with our previous observations, we can compare measured and computed profiles of plasma density, velocity, and magnetic filed jumps across the IP shock.

Profiles of magnetic field and plasma parameters across a shock in the magnetosheath

For comparison of measurements with models we have chosen the already discussed event — May 18, 1999 (*Koval et al.*, 2005d) [A5].

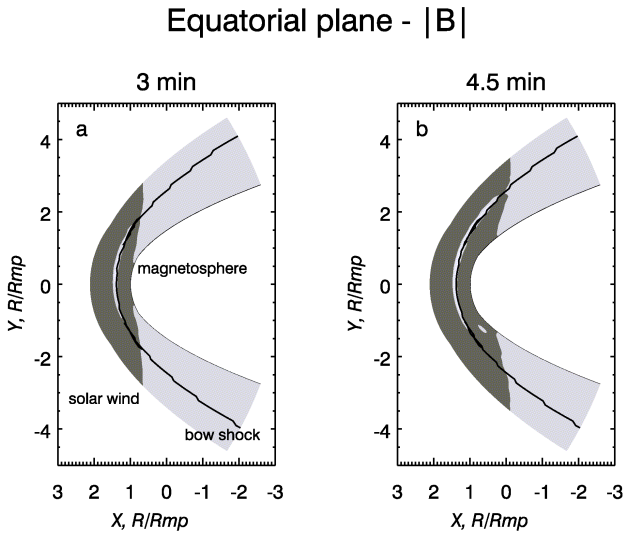

Figure 7: MHD modeling of a weak IP shock and its propagation in the MSH. Model shock parameters before the shock: $n = 5$ cm^{-3}; $V_x = 400$ km/s; $V_y = V_z = 0; T_i = 2.4 \cdot 10^5; |B| = 5$ nT; the angle in the X-Y plane = 45^o and the shock jumps: $B_2/B_1 = 1.24; n_2/n_1 = 1.2; T_2/T_1 = 2.7; V_{x2}/V_{x1} = 1.07$; the shock velocity = 568 km/s; and Alfvén Mach number = 3.4. Subscripts 1 and 2 correspond to upstream and downstream values of all parameters. The light area is before the shock ($B/B_0 \sim 1$) and the dark area is after the shock when $B/B_0 > 1$.

Multi-spacecraft observations of the shock passage in the solar wind indicate that profiles of the magnetic filed and plasma parameters are similar at different locations (Figure 5). However, the magnetosheath profiles differ significantly from those observed in the solar wind: the jumps of the magnetosheath parameters are not as sharp as in the solar wind and there are overshoots of the magnetosheath proton number density and bulk velocity which are not observed in the solar wind.

In order to understand the difference between the behavior of the solar wind and magnetosheath parameters, we simulated the magnetosheath parameters using two MHD models: the 3-D global BATS-R-US (Block-Adaptive-Tree-Solar wind-Roe-Upwind-Scheme) model (*Groth et al.*, 2000) and a 3-D local magnetosheath model (*Samsonov*, 2005). The comparison of the model predictions with observations is presented in Figure 8. The black thick lines show the Geotail data; the BATS-R-US computations are shown by dashed lines; gray and black thin lines show the two results from the local magnetosheath model — with solid (gray line) and movable (black line) inner boundaries. The comparison with the data reveals a good coincidence between the predicted and observed times of the shock passage, indicating that both models predict the observed deceleration of the shock in the magnetosheath. Differences in timing among models are small and they are attributed to the differing grid resolutions. The main difference between the models is the behavior of the IMF B_z component (last panel) that is nearly zero in the BATS-R-US computation. Profiles provided by the local magnetosheath model are more similar to the observations. The fluctuations observed in the post-shock interval are probably caused by the magnetopause reaction and thus their forms differ in the two versions of the local model.

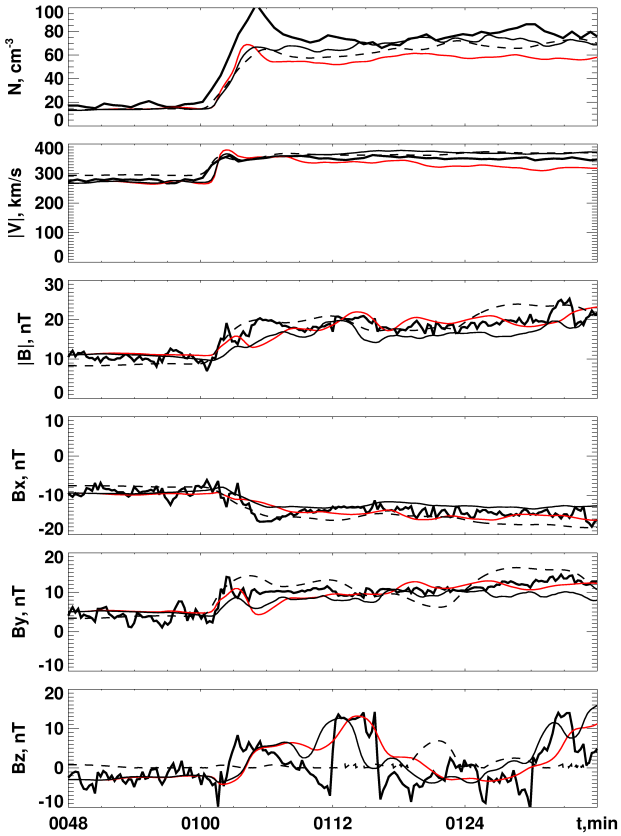

Figure 8: A comparison of Geotail magnetosheath observations with the BATS-R-US and a local magnetosheath model predictions (from top to bottom: densities, speeds, magnetic field magnitudes, and magnetic field components).

All the modeled pre-shock magnetosheath values in Figure 8 are very close to those observed. The local magnetosheath model (both versions) gives a better match, probably because this model uses an approximation of the magnetopause surface obtained from the *Shue et al.* (1998) empirical model, whereas the BATS-R-US magnetopause is built self-consistently under simplified assumptions. The same is true for the post-shock interval.

The most interesting results were obtained for the interval immediately following the IP shock ramp (0100 – 0112 UT). All models predict an overshoot in the plasma velocity profile that is consistent with the observations. The observed density overshoot, however, is much larger than the model predictions. The most distinct overshoot is predicted by the local magnetosheath model with a solid obstacle (gray thin line in Figure 8), whereas the overshoot is missing in the same model with the movable obstacle (black thin line). This difference suggests that the presence of the overshoot is connected with the magnetopause reaction to the pressure pulse. The height of the overshoot is underestimated in all models and thus it may be connected with non-MHD effects.

Finally, we would like to conclude that both MHD models well reproduce the observed pre- and post-shock conditions as well as the steepness of the shock front in the magnetosheath. We did not find any significant differences in the plasma parameters predicted by the BATS-R-US model and two versions of local magnetosheath model. A comparison of two versions of the local model showed that the overshoot of the plasma

density is caused by a delay in the magnetopause reaction to the increase of the upstream pressure. The good overall agreement between the measured and modeled data suggests that MHD effects dominate over kinetic effects even in the vicinity of the magnetopause.

Conclusion

The thesis deals with the propagation of solar wind discontinuities through the solar wind and their interaction with the Earth's bow shock. Two main topics are discussed: (1) interaction of IMF tangential discontinuities with the bow shock and properties of resulting HFAs, and (2) propagation of IP shocks through the solar wind, their interaction with the bow shock and modification of their parameters in the magnetosheath.

To detect a motion and gradual evolution of solar wind structures, we used simultaneous multipoint observations by the Wind, ACE, SOHO, Geotail, IMP 8, and Interball-1/MAGION-4 spacecraft located in all crucial regions: far upstream in the solar wind, in the vicinity of the Earth's bow shock, and in the magnetosheath. To determine particular ion flow parameters (three components of the velocity vector, temperature, and density) from the ion flux measurements by the Faraday's cups of the omnidirectional plasma sensor VDP onboard Interball-1, we have developed new methods based on a comparison of actual observations with model results of the instrumental response for various sets of ion flow parameters assuming an isotropic Maxwellian velocity distribution. We also used the advantages of a high-time resolution of ion flux measurements by Faraday's cups and a possibility to compute plasma parameters from them to develop a small fast solar wind monitor for the SPECTR-R project (*Koval et al.*, 2005a) [A1].

The ion flow parameters computed from the measurements of the VDP instrument onboard the Interball-1 spacecraft were used for analysis of the relationship between the ion flow inside HFA cavities and orientations of an IMF tangential discontinuity (*Koval et al.*, 2005b) [A2]. Our results show that, beside the dominant plasma motion connected with the sweeping of the discontinuity, a significant velocity component directed along the discontinuity can be found. This suggests a highly elongated shape of the HFA cavity. Such shape can explain very different durations of HFA observations which range from seconds to tens of minutes. The correlation length of particular HFA features (amplitude of bounding density enhancements, their durations, etc.) may be rather short; it is of the order of 1 R_E in our case. We also suggest that HFA which extends into the magnetosheath modifies locally downstream the Mach number and causes a local displacement of the bow shock.

The importance of an accurate determination of the parameters associated with the gradual evolution of IP shocks in the solar wind and their transmissions through the magnetosheath to the magnetosphere boundary led us to a detail study of propagation of an IP shock observed by multiple spacecraft in the solar wind and by at least one spacecraft located in the magnetosheath.

Multi-spacecraft observations of the shock passage in the solar wind indicate that the shock parameters are generally similar at different locations there and the corresponding magnetosheath shock-like discontinuity has characteristics of the original MHD shock. However, we have also demonstrated a possibility of an IP shock evolution into a slow IMF rotation while propagating through the solar wind towards the Earth's bow shock

and its transformation into another type of the MHD shock after an interaction with the Earth's bow shock (*Koval et al.*, 2004) [A3].

Among the multispacecraft observations, those events for which the passage of the shock is observed by at least four spacecraft located in the solar wind have significant advantages. Assumption of a planar shock geometry for these cases allows calculation of global shock parameters directly from the times of shock identifications by the particular spacecraft. In the time interval from 1995–1999, we have identified 10 IP shocks which satisfy this criterion. Our investigation of propagation of these shocks through the magnetosheath brings the evidence that IP shocks slightly decelerate there contrary to a gasdynamic prediction (*Koval et al.*, 2005c) [A4]. Therefore, we have modeled the propagation of IP shocks in the magnetosheath using two MHD models (the 3-D global BATS-R-US model (*Groth et al.*, 2000) and a 3-D local magnetosheath model (*Samsonov and Hubert*, 2004; *Samsonov*, 2005)) and showed that the observation of shock deceleration agrees with model predictions (*Koval et al.*, 2005c,d) [A4, A5]. Our MHD modeling suggests that the speed of the shock front propagation in the magnetosheath decreases from the bow shock toward the magnetopause and the front of the IP shock deforms. These MHD models also well reproduce magnetic field and plasma parameter profiles across the shock in the magnetosheath, although they are different from those in the solar wind (*Koval et al.*, 2005d) [A5]. The good overall agreement between measured and modeled profiles suggests that MHD effects dominate over kinetic effects in these interactions.

Finally, we would like to note that the propagation of solar wind discontinuities in the solar wind as well as in the magnetosheath is a complex problem and its investigation is not a simple task. Our results implicate that the assumption of the shock planarity in the magnetosheath should be abandoned and it makes this task even more complicated. Moreover, our as well as previous MHD modeling suggests that the interaction of an IP shock with the bow shock creates a train of new discontinuities and this fact would influence the IP shock arrival to the magnetopause. We think that our investigations contributed to a solution of these problems but much more items remain for further studies.

Acknowledgments. The present work was supported by the Czech Grant Agency under Contracts *No.* 205/02/0947, 205/03/0953, 202/03/H162, 205/05/0170, by the Czech Ministry of Education grant ME-648, by the Research Projects of the Czech Ministry of Education MSM 113200004, by the INTAS grant for young scientists 03-55-1034, by RFBR grant 03-05-64865, and by the USA NSF grants ATM-0207775 and ATM-0203723.

References

Bellomo, A., and A. Mavretic (1978), Description of the MIT plasma experiment on IMP 7/8, in *Rep. CSR TR-78-2, Cent. for Space Res., MIT, Cambridge*, p. 51.

Burgess, D. (1989), On the effect of a tangential discontinuity on ions specularly reflected at an oblique shock, *J. Geophys. Res.*, *94*, 472–478.

Ciobanu, M. I., and A. Moldovanu (1995), SGR 8 magnetometer for the Tail probe and Auroral probe satellites, in *INTERBALL Mission and Payload*, edited by Y. Galperin, pp. 230–232, CNES–IKI–RSA.

Dryer, M. (1973), Bow shock and its interaction with interplanetary shocks, *Radio Science*, *8*(11), 893–901.

Frank, L. A., K. L. Ackerson, W. R. Paterson, J. A. Lee, M. R. English, and G. L. Pickett (1994), The Comprehensive Plasma Instrumentation (CPI) for the Geotail spacecraft, *J. Geomagn. Geoelectr.*, *46*, 7–21.

Groth, C. P. T., D. L. De Zeeuw, T. I. Gombosi, and K. G. Powell (2000), Global three-dimensional MHD simulation of a space weather event: CME formation, interplanetary propagation, and interaction with the magnetosphere, *J. Geophys. Res.*, *105*, 25,053–25,078, doi: 10.1029/2000JA900093.

Ipavich, F. M., A. B. Galvin, S. E. Lasley, J. A. Paquette, S. Hefti, K.-U. Reiche, M. A. Coplan, G. Gloeckler, P. Bochsler, D. Hovestadt, H. Grünwaldt, M. Hilchenbach, F. Gliem, W. I. Axford, H. Balsiger, A. Bürgi, J. Geiss, K. C. Hsieh, R. Kallenbach, B. Klecker, M. A. Lee, G. G. Managadze, E. Marsch, E. Möbius, M. Neugebauer, M. Scholer, M. I. Verigin, B. Wilken, and P. Wurz (1998), Solar wind measurements with SOHO: The CELIAS/MTOF proton monitor, *J. Geophys. Res.*, *103*, 17,205–17,214, doi:10.1029/97JA02770.

Jeřáb, M., Z. Němeček, J. Šafránková, K. Jelínek, and J. Měrka (2005), Improved bow shock model with dependence on the IMF strength, *Planet. Space Sci.*, *53*, 85–93, doi: 10.1016/j.pss.2004.09.032.

Klimov, S., S. Romanov, E. Amata, J. Blecki, J. Büchner, J. Juchniewicz, J. Rustenbach, P. Triska, L. J. C. Woolliscroft, S. Savin, Y. Afanas'yev, U. de Angelis, U. Auster, G. Bellucci, A. Best, F. Farnik, V. Formisano, P. Gough, R. Grard, V. Grushin, G. Haerendel, V. Ivchenko, V. Korepanov, H. Lehmann, B. Nikutowski, M. Nozdrachev, S. Orsini, M. Parrot, A. Petrukovich, J. L. Rauch, K. Sauer, A. Skalsky, J. Slominski, J. G. Trotignon, J. Vojta, and R. Wronowski (1997), ASPI experiment: measurements of fields and waves on board the INTERBALL-1 spacecraft, *Annales Geophysicae*, *15*, 514–527.

Kokubun, S., T. Yamamoto, M. H. Acuna, K. Hayashi, K. Shiokawa, and H. Kawano (1994), The Geotail magnetic field experiment, *J. Geomagn. Geoelectr.*, *46*, 7–21.

Koval, A., J. Šafránková, Z. Němeček, and L. Přech (2004), Propagation of interplanetary shocks through the solar wind and magnetosheath, submitted to *Advances in Space Research*.

Koval, A., Z. Němeček, J. Šafránková, K. Jelínek, M. Beránek, G. Zastenker, and N. Shevyrev (2005a), The proposal of a small fast solar wind monitor for the SPECTR-R project, in *Proc. Solar Wind 11 – SOHO 16*, pp. 681–684.

Koval, A., J. Šafránková, and Z. Němeček (2005b), A study of particle flows in hot flow anomalies, *Planet. Space Sci.*, *53*, 41–52, doi:10.1016/j.pss.2004.09.027.

Koval, A., J. Šafránková, Z. Němeček, L. Přech, A. A. Samsonov, and J. D. Richardson (2005c), Deformation of interplanetary shock fronts in the magnetosheath, *Geophys. Res. Lett.*, *32*, 15,101, doi:10.1029/2005GL023009.

Koval, A., J. Šafránková, Z. Němeček, A. A. Samsonov, L. Přech, J. D. Richardson, and M. Hayosh (2005d), Interplanetary shock in the magnetosheath: Comparison of experimental data with MHD modeling, submitted to *Geophys. Res. Lett.*

Lepping, R. P., M. H. Acuna, L. F. Burlaga, W. M. Farrell, J. A. Slavin, K. H. Schatten, F. Mariani, N. F. Ness, F. M. Neubauer, Y. C. Whang, J. B. Byrnes, R. S. Kennon, P. V. Panetta, J. Scheifele, and E. M. Worley (1995), The Wind Magnetic Field Investigation, *Space Science Reviews*, *71*, 207–229.

Lin, R. P., K. A. Anderson, S. Ashford, C. Carlson, D. Curtis, R. Ergun, D. Larson, J. McFadden, M. McCarthy, G. K. Parks, H. Reme, J. M. Bosqued, J. Coutelier, F. Cotin, C. D'Uston, K.-P. Wenzel, T. R. Sanderson, J. Henrion, J. C. Ronnet, and G. Paschmann (1995), A Three-Dimensional Plasma and Energetic Particle Investigation for the Wind Spacecraft, *Space Science Reviews*, *71*, 125–153.

Lin, Y. (1997), Generation of anomalous flows near the bow shock by its interaction with interplanetary discontinuities, *J. Geophys. Res.*, *102*, 24,265–24,282, doi:10.1029/97JA01989.

McComas, D. J., S. J. Bame, P. Barker, W. C. Feldman, J. L. Phillips, P. Riley, and J. W. Griffee (1998), Solar Wind Electron Proton Alpha Monitor (SWEPAM) for the Advanced Composition Explorer, *Space Science Reviews*, *86*, 563–612.

Nozdrachev, M. N., A. A. Skalsky, V. A. Styazhkin, and V. G. Petrov (1998), Some Results of Magnetic Field Measurements by the FM-3I Flux-Gate Instrument Onboard the INTERBALL-1 Spacecraft, *Cosmic Research*, *36*, 251.

Ogilvie, K. W., D. J. Chornay, R. J. Fritzenreiter, F. Hunsaker, J. Keller, J. Lobell, G. Miller, J. D. Scudder, E. C. Sittler, R. B. Torbert, D. Bodet, G. Needell, A. J. Lazarus, J. T. Steinberg, J. H. Tappan, A. Mavretic, and E. Gergin (1995), SWE, A Comprehensive Plasma Instrument for the Wind Spacecraft, *Space Science Reviews*, *71*, 55–77.

Paschmann, G., G. Haerendel, N. Sckopke, E. Moebius, and H. Luehr (1988), Three-dimensional plasma structures with anomalous flow directions near the earth's bow shock, *J. Geophys. Res.*, *93*, 11,279–11,294.

Petrinec, S. M., and C. T. Russell (1996), Near-Earth magnetotail shape and size as determined from the magnetopause flaring angle, *J. Geophys. Res.*, *101*, 137–152, doi:10.1029/95JA02834.

Russell, C. T., M. M. Mellott, E. J. Smith, and J. H. King (1983), Multiple spacecraft observations of interplanetary shocks Four spacecraft determination of shock normals, *J. Geophys. Res.*, *88*, 4739–4748.

Russell, C. T., Y. L. Wang, J. Raeder, R. L. Tokar, C. W. Smith, K. W. Ogilvie, A. J. Lazarus, R. P. Lepping, A. Szabo, H. Kawano, T. Mukai, S. Savin, Y. I. Yermolaev, X.-Y. Zhou, and B. T. Tsurutani (2000), The interplanetary shock of September 24, 1998: Arrival at Earth, *J. Geophys. Res.*, *105*, 25,143–25,154, doi:10.1029/2000JA900070.

Samsonov, A. A. (2005), Numerical modeling of the Earth's magnetosheath for different IMF orientations, *Advances in Space Research*, doi:10.1016/j.asr.2005.06.009.

Samsonov, A. A., and D. Hubert (2004), Steady state slow shock inside the Earth's magnetosheath: To be or not to be? 2. Numerical three-dimensional MHD modeling, *J. Geophys. Res.*, *109*, 1218, doi:10.1029/2003JA010006.

Schwartz, S. J. (1995), Hot flow anomalies near the Earth's bow shock, *Advances in Space Research*, *15*, 107–116.

Schwartz, S. J., C. P. Chaloner, D. S. Hall, P. J. Christiansen, and A. D. Johnstones (1985), An active current sheet in the solar wind, *Nature*, *318*, 269–271.

Schwartz, S. J., R. L. Kessel, C. C. Brown, L. J. C. Woolliscroft, and M. W. Dunlop (1988), Active current sheets near the earth's bow shock, *J. Geophys. Res.*, *93*, 11,295–11,310.

Schwartz, S. J., G. Paschmann, N. Sckopke, T. M. Bauer, M. Dunlop, A. N. Fazakerley, and M. F. Thomsen (2000), Conditions for the formation of hot flow anomalies at Earth's bow shock, *J. Geophys. Res.*, *105*, 12,639–12,650, doi:10.1029/1999JA000320.

Shue, J.-H., P. Song, C. T. Russell, J. T. Steinberg, J. K. Chao, G. Zastenker, O. L. Vaisberg, S. Kokubun, H. J. Singer, T. R. Detman, and H. Kawano (1998), Magnetopause location under extreme solar wind conditions, *J. Geophys. Res.*, *103*, 17,691–17,700, doi:10.1029/98JA01103.

Sibeck, D. G., N. L. Borodkova, S. J. Schwartz, C. J. Owen, R. Kessel, S. Kokubun, R. P. Lepping, R. Lin, K. Liou, H. Lühr, R. W. McEntire, C.-I. Meng, T. Mukai, Z. Nemecek, G. Parks, T. D. Phan, S. A. Romanov, J. Safrankova, J.-A. Sauvaud, H. J. Singer, S. I. Solovyev, A. Szabo, K. Takahashi, D. J. Williams, K. Yumoto, and G. N. Zastenker (1999), Comprehensive study of the magnetospheric response to a hot flow anomaly, *J. Geophys. Res.*, *104*, 4577–4594, doi:10.1029/1998JA900021.

Smith, C. W., J. L'Heureux, N. F. Ness, M. H. Acuña, L. F. Burlaga, and J. Scheifele (1998), The ACE Magnetic Fields Experiment, *Space Science Reviews*, *86*, 613–632.

Spreiter, J. R., and S. S. Stahara (1992), Computer modeling of solar wind interaction with Venus and Mars, *Washington DC American Geophysical Union Geophysical Monograph Series*, *66*, 345–383.

Szabo, A. (2004), Interplanetary discontinuities and shocks in the Earths magnetosheath, in *Multiscale Processes in the Earths Magnetosphere: From Interball to Cluster,*, edited by J.-A. Sauvaud and Z. Nemecek, pp. 57–71.

Szabo, A. (2005), Determination of interplanetary shock characteristics, in *Proc. Solar Wind 11 – SOHO 16*, pp. 449–452.

Szabo, A., C. W. Smith, and R. M. Skough (2000), The transition of interplanetary shocks through the magnetosheath, *EOS Supp.*, *81*, F966.

Szabo, A., R. P. Lepping, J. Merka, C. W. Smith, and R. M. Skoug (2001), The evolution of interplanetary shocks driven by magnetic clouds, in *ESA SP-493: Solar encounter. Proceedings of the First Solar Orbiter Workshop*, pp. 383–387.

Šafránková, J., G. Zastenker, Z. Němeček, A. Fedorov, M. Simersky, and L. Přech (1997), Small scale observation of magnetopause motion: preliminary results of the INTERBALL project, *Annales Geophysicae*, *15*, 562–569.

Šafránková, J., Z. Němeček, L. Přech, G. Zastenker, K. I. Paularena, N. Nikolaeva, M. Nozdrachev, A. Skalsky, and T. Mukai (1998), The January 10-11, 1997 magnetic cloud: Multipoint measurements, *Geophys. Res. Lett.*, *25*, 2549–2552, doi:10.1029/98GL50330.

Šafránková, J., L. Přech, Z. Němeček, D. G. Sibeck, and T. Mukai (2000), Magnetosheath response to the interplanetary magnetic field tangential discontinuity, *J. Geophys. Res.*, *105*, 25,113–25,122, doi:10.1029/1999JA000435.

Šafránková, J., L. Přech, Z. Němeček, and D. Sibeck (2002), The structure of hot flow anomalies in the magnetosheath, *Advances in Space Research*, *30*, 2737–2744.

Thomas, V. A., D. Winske, M. F. Thomsen, and T. G. Onsager (1991), Hybrid simulation of the formation of a hot flow anomaly, *J. Geophys. Res.*, *96*, 11,625.

Thomsen, M. F., J. T. Gosling, S. A. Fuselier, S. J. Bame, and C. T. Russell (1986), Hot, diamagnetic cavities upstream from the earth's bow shock, *J. Geophys. Res.*, *91*, 2961–2973.

Thomsen, M. F., J. T. Gosling, S. J. Bame, K. B. Quest, and C. T. Russell (1988), On the origin of hot diamagnetic cavities near the earth's bow shock, *J. Geophys. Res.*, *93*, 11,311–11,325.

Villante, U., S. Lepidi, P. Francia, and T. Bruno (2004), Some aspects of the interaction of interplanetary shocks with the Earth's magnetosphere: an estimate of the propagation time through the magnetosheath, *J. Atmosph. Sol.-Terr. Phys.*, *66*, 337.

Whang, Y. C. (1991), Shock interactions in the outer heliosphere, *Space Science Reviews*, *57*, 339–388.

Yan, M., and L. C. Lee (1996), Interaction of interplanetary shocks and rotational discontinuities with the Earth's bow shock, *J. Geophys. Res.*, *101*, 4835–4848, doi:10.1029/95JA02976.

Zhuang, H. C., and C. T. Russell (1981), An analytic treatment of the structure of the bow shock and magnetosheath, *J. Geophys. Res.*, *86*, 2191–2205.

Zhuang, H. C., C. T. Russell, E. J. Smith, and J. T. Gosling (1981), Three-dimensional interaction of interplanetary shock waves with the bow shock and magnetopause — A comparison of theory with ISEE observations, *J. Geophys. Res.*, *86*, 5590–5600.

Papers included in the thesis

A1: Koval, A., Z. Němeček, J. Šafránková, K. Jelínek, M. Beránek, G. Zastenker, and N. Shevyrev (2005), The proposal of a small fast solar wind monitor for the SPECTR-R project, in *Proc. Solar Wind 11 – SOHO 16*, pp. 681–684.

A2: Koval, A., J. Šafránková, and Z. Němeček (2005), A study of particle flows in hot flow anomalies, *Planet. Space Sci., 53*, 41–52, doi:10.1016/j.pss.2004.09.027.

A3: Koval, A., J. Šafránková, Z. Němeček, and L. Přech (2004), Propagation of interplanetary shocks through the solar wind and magnetosheath, submitted to *Adv. Space Res.*

A4: Koval, A., J. Šafránková, Z. Němeček, L. Přech, A. A. Samsonov, and J. D. Richardson (2005), Deformation of interplanetary shock fronts in the magnetosheath, *Geophys. Res. Lett., 32*, 15,101, doi:10.1029/2005GL023009.

A5: Koval, A., J. Šafránková, Z. Němeček, A. A. Samsonov, L. Přech, J. D. Richardson, and M. Hayosh (2005), Interplanetary shock in the magnetosheath: Comparison of experimental data with MHD modeling, submitted to *Geophys. Res. Lett.*

Other papers related to the topic

1. Dobreva, P., N. Shevyrev, A. Koval, M. Kartalev, G. Zastenker (2006), Interpretation of satellite magnetosheath plasma measurements by use of a magnetosheath-magnetosphere numerical model, submitted to *Journal of Theoretical and Applied Mechanics*.

2. Koval, A., J. Šafránková, Z. Němeček, G. Zastenker, N. Shevyrev (2003), Proposal of a small solar wind monitor and method of plasma parameter determination, in *WDS'03 Proceedings of Contributed Papers: Part II - Physics of Plasmas and Ionized Media*, edited by J. Šafránková, pp. 270-275, Prague, Matfyzpress.

3. Koval, A., J. Šafránková, Z. Němeček, L. Přech (2004), Significant Magnetosheath Disturbances and Their Upstream Counterparts, in *WDS'04 Proceedings of contributed papers: Part II - Physics of Plasmas and Ionized Media*, edited by J. Šafránková, pp. 229-235, Prague, Matfyzpress.

4. Koval, A., J. Šafránková, Z. Němeček, L. Přech, and M. Hayosh (2005), Evolution of an interplanetary shock in the magnetosheath, *in WDS'05 Proceedings of contributed papers: Part II - Physics of Plasmas and Ionized Media*, edited by J. Šafránková, pp. 220-224, Prague, Matfyzpress.